
Contrastive Diffuser: Planning Towards High Return States via Contrastive Learning

Yixiang Shan¹ Zhengbang Zhu² Ting Long¹ Qifan Liang¹ Yi Chang¹ Weinan Zhang² Liang Yin²

Abstract

Applying diffusion models in reinforcement learning for long-term planning has gained much attention recently. Several diffusion-based methods have successfully leveraged the modeling capabilities of diffusion for arbitrary distributions. These methods generate subsequent trajectories for planning and have demonstrated significant improvement. However, these methods are limited by their plain base distributions and their overlooking of the diversity of samples, in which different states have different returns. They simply leverage diffusion to learn the distribution of offline dataset, generate the trajectories whose states share the same distribution with the offline dataset. As a result, the probability of these models reaching the high-return states is largely dependent on the dataset distribution. Even equipped with the guidance model, the performance is still suppressed. To address these limitations, in this paper, we propose a novel method called CDiffuser, which devises a return contrast mechanism to pull the states in generated trajectories towards high-return states while pushing them away from low-return states to improve the base distribution. Experiments on 14 commonly used D4RL benchmarks demonstrate the effectiveness of our proposed method.

Recently, some offline RL methods have incorporated diffusion for long-term planning, showcasing effectiveness and attracting considerable attention. Taking advantages of diffusion models (Song et al.; 2020; Ho et al., 2020), they generalize the distribution of the offline dataset and enhance the performance significantly. Specifically, these methods leverage the diffusion model to generate the distribution of the subsequent trajectory (we name this distribution as **the base distribution**), and further apply the classifier guidance (Dhariwal & Nichol, 2021) over the base distribution to obtain a high-return trajectory, which contains the action to be taken. In this process, the state-action pairs in the generated trajectory carry the planned future information and act as a condition for decision-making. As a result, these methods achieve outstanding performance in many tasks.

However, existing methods introducing diffusion models are limited by their plain base distributions and their neglecting of the diversity of samples in offline datasets. The classifier-guided sampling process of these methods can be viewed as sampling from a weighted average of two distributions: the base distribution and the distribution of the classifier guidance (Janner et al., 2022; Ada et al., 2023; Dhariwal & Nichol, 2021). Their base distributions are highly close to the dataset distribution, which makes these methods sensitive to the proportions of suboptimal samples in the dataset (Yue et al., 2022; Wang et al., 2022; Chen et al., 2023). As shown in Figure 1, the base distribution (b), where the generated trajectories are samples from, is similar to the original distribution of the offline dataset (a), making the probability of sampling high-return states restricted if there are many low-return states in the dataset. Even with classifier guidance (Dhariwal & Nichol, 2021) techniques to enforce the generation towards the high-return area, the results remain unsatisfactory as depicted in Figure 1(c). Although the sampling distribution is more concentrated within the guidance circle, there are still many samples spread over the entire low-return area, which may cause many low-return states in the generated trajectories. Intuitively, if constraining the base distribution to be close to the area with high-return states and away from the area with low-return states, like Figure 1 (d), we would obtain better results under the guidance, like Figure 1(e).

1. Introduction

Offline reinforcement learning (offline RL) (Levine et al., 2020; Prudencio et al., 2023) is a significant branch of reinforcement learning, where an agent is trained on pre-collected offline datasets and is evaluated online. Since offline RL avoids potential risks from interacting with the environment during policy learning, it has broad applications in numerous real-world scenarios, like commercial recommendation (Xiao & Wang, 2021), health care (Fatemi et al., 2022), dialog (Jaques et al., 2020), and autonomous driving (Shi et al., 2021).

¹Jilin University, China ²Shanghai Jiaotong University, China. Correspondence to: Ting Long <longting@jlu.edu.cn>, Yi Chang <yichang@jlu.edu.cn>.

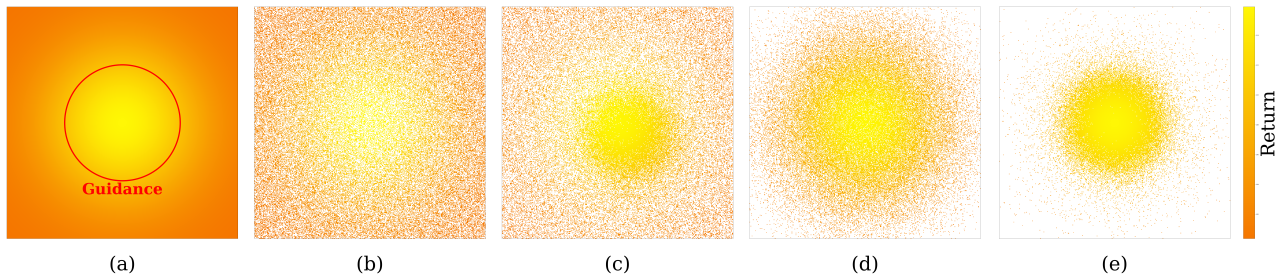


Figure 1. Comparison of different distributions: (a) The dataset distribution; (b) The base distribution; (c) The distribution of classifier guide sampling; (d) The improved base distribution; (e) The improved distribution of classifier guide sampling. Each scatter in sub-figure represents a two-dimensional state, and the color of each scatter denotes the corresponding return.

Considering contrastive learning (CL) (Khosla et al., 2020; Yeh et al., 2022) is designed for pulling a sample towards similar samples and pushing it away from dissimilar samples, which is analogous to the case of pulling the states in the generated trajectory towards the high-return areas and away from low-return areas, we introduce contrastive learning to diffusion-based RL methods and propose a novel method called **Contrastive Diffuser (CDiffuser)**. Different from the previous works (Qiu et al., 2022; Laskin et al., 2020; Yuan & Lu, 2022; Agarwal et al., 2020) which leverage CL for the representation learning in RL, we introduce CL to improve the base distribution of diffusion-based RL method with contrastive mechanism. Specifically, we group the states in the offline dataset into high-return states and low-return states in a soft manner. Then, we learn a diffusion-based trajectory generation model to generate the trajectories whose states are constrained by contrastive learning. In such manner, the base distribution (see Figure 1(b)) is enhanced. As a result, the states in generated trajectories closely align with high-return states while staying away from low-return states. With the help of contrastive learning, CDiffuser generates better trajectories for planning. To evaluate the performance of CDiffuser, we conduct experiments on 14 D4RL benchmarks (Fu et al., 2020). The experiment results demonstrate that CDiffuser has superior performance.

In summary, our contributions are: (i) We propose a method called CDiffuser, which novelly improves the base distribution of diffusion-based RL methods and achieves outstanding performance, providing an innovative perspective of improving diffusion-based RL methods for the subsequent works. (ii) We perform contrastive learning over returns of states to improve the base distribution. To the best of our knowledge, our work is the first which notices the limitation of the base distribution, and the first which applies contrastive learning to enhance the base distribution for diffusion based RL methods. (iii) Experiment results on 14 D4RL datasets demonstrate the outstanding performance of CDiffuser.

2. Preliminaries

2.1. Denoising Probabilistic Models

Denoising Probabilistic Models (Diffusion Models) (Sohl-Dickstein et al., 2015; Song et al.; Ho et al., 2020) are a group of generative models, which generate samples by denoising from Gaussian noise. A diffusion model is composed of a forward process and a backward process. Given the original data $\mathbf{x} \sim q(\mathbf{x})$, the forward process transfers \mathbf{x} into Gaussian noise by gradually adding noise, i.e., $q(\mathbf{x}^i | \mathbf{x}^{i-1}) = \mathcal{N}(\mathbf{x}^i; \sqrt{1 - \beta^i} \mathbf{x}^{i-1}, \beta^i \mathbf{I})$, in which \mathbf{I} is an identity matrix, β^i is the noise schedule measuring the proportion of noise added at each step, $\mathbf{x}^0 := \mathbf{x}$ is a sample from the offline dataset, $\mathbf{x}^1, \mathbf{x}^2, \dots$ are the latents of diffusion. The backward process recovers \mathbf{x} by gradually removing the noise at each step, which is formulated with a Gaussian distribution (Feller, 1949) parameterized by θ , i.e., $p_\theta(\mathbf{x}^{i-1} | \mathbf{x}^i) = \mathcal{N}(\mu_\theta(\mathbf{x}^i, i), \Sigma_\theta(\mathbf{x}^i, i))$, where $\mu_\theta(\mathbf{x}^i, i) = \frac{\sqrt{\bar{\alpha}^i(1-\bar{\alpha}^i)}}{1-\bar{\alpha}^{i-1}} \mathbf{x}^i + \frac{\sqrt{\bar{\alpha}^{i-1}\beta^i}}{1-\bar{\alpha}^i} \psi_\theta(\mathbf{x}^i, i)$, $\bar{\alpha}^i = \prod_{j=1}^i (1 - \beta^j)$ and $\psi_\theta(\cdot, \cdot)$ is a model to reconstruct \mathbf{x} . The objective function can be formulated as follows if we fix $\Sigma_\theta(\mathbf{x}_t, t) = \beta_t \mathbf{I}$ (Ho et al., 2020):

$$\mathcal{L} = \mathbb{E}_{\mathbf{x}^0, i \sim [1, N]} [\|\mathbf{x}^0 - \psi_\theta(\mathbf{x}^i, i)\|^2]. \quad (1)$$

2.2. Contrastive Learning

Contrastive learning (Schroff et al., 2015; Sohn, 2016; Khosla et al., 2020; Yeh et al., 2022; Oord et al., 2018) is a class of self-supervised learning methods which aim at pulling similar samples together and pushing dissimilar samples away from each other. Specifically, given a sample \mathbf{x} and a similarity measure, the positive set \mathcal{S}^+ is defined as the collection of samples similar to \mathbf{x} , while the negative set \mathcal{S}^- is defined as the collection of samples dissimilar to \mathbf{x} . Contrastive learning minimizes the distance of between \mathbf{x} and \mathcal{S}^+ , and maximizes the distance of \mathbf{x} and \mathcal{S}^- . That is, for each sample \mathbf{x} , select a positive sample $\mathbf{x}^+ \in \mathcal{S}^+$ and negative samples $\mathbf{x}^- \in \mathcal{S}^-$. We have:

$$\mathcal{L} = -\log \left[\frac{\exp(\text{sim}(f(\mathbf{x}), f(\mathbf{x}^+)))}{\exp(\text{sim}(f(\mathbf{x}), f(\mathbf{x}^+))) + \sum_{\mathbf{x}^- \in \mathcal{S}^-} \exp(\text{sim}(f(\mathbf{x}), f(\mathbf{x}^-)))} \right], \quad (2)$$

where $f(\cdot)$ denotes the function to map samples to a latent space and $\text{sim}(\cdot, \cdot)$ denotes the similarity measure.

2.3. Problem Definition

Considering a system composed of three parts: policy, agent, and environment. The environment in RL is usually formulated as a Markov Decision Process (MDP) (Sutton & Barto, 2018) $\mathcal{M} = \{\mathcal{S}, \mathcal{A}, \mathcal{P}, r, \gamma\}$, where \mathcal{S} is the state space, \mathcal{A} is the action space, $\mathcal{P}(s'|s, a)$ is the transition function, γ represents the discount factor, r is the instant reward of each step. At each step t , the agent responds to the state of environment s_t by action a_t according to policy π_θ parameterized by θ , and gets an instant return r_t . The interaction history is formulated as a trajectory $\tau = \{(s_t, a_t, r_t) | t \geq 0\}$. In this paper, we define the cumulative discounted reward from step t as $v_t = \sum_{i \geq t} \gamma^{i-t} r_i$ and call it the return of s_t .

We focus on the offline RL setting in this paper. Therefore, given an offline dataset $\mathcal{D} \triangleq \{(s_t, a_t, r_t, s_{t+1}) | t \geq 0\}$ consisting of transition tuples, and defining the return of trajectory τ as $R(\tau) \triangleq \sum_{t \geq 0} \gamma^t r_t$, our goal is learning π_θ to maximize the expected return without directly interacting with the environment, *i.e.*,

$$\pi_\theta = \arg \max_{\theta} \mathbb{E}_{\tau \sim \pi_\theta} [R(\tau)]. \quad (3)$$

3. Methodology

We formulate the offline RL problem as a state-conditioned sequence generative task in the light of previous works (Janer et al., 2022; Ajay et al., 2023). To improve the base distribution, we propose a method called Contrastive Diffuser (CDiffuser), which introduces contrastive learning in offline RL and adopts a contrastive mechanism to effectively harnessing the inherent information within the dataset distribution. Specifically, our CDiffuser is composed of two modules: (1) the Planning Module, which aims to generate subsequent trajectories; (2) the Contrastive Module, which is designed to keep the states in generated trajectories within the high-return areas and away from low-return areas, as is illustrated in Figure 2.

3.1. Planning Module

Given a state s_t at step t , the Planning Module estimates v_t as guidance, leverages the guidance as well as s_t as the condition to generate the subsequent trajectory $\hat{\tau}_t^0$, and then extract the action to be executed from $\hat{\tau}_t^0$, as is illustrated in Figure 2. Specifically, we first sample $\hat{\tau}_t^N$ from $\mathcal{N}(\mathbf{0}, \mathbf{I})$, and replace \hat{s}_t^N with s_t as condition on the current observation:

$$\hat{\tau}_t^N = \{(s_t, \hat{a}_t^N), (\hat{s}_{t+1}^N, \hat{a}_{t+1}^N), \dots, (\hat{s}_{t+H}^N, \hat{a}_{t+H}^N)\}, \quad (4)$$

in which all the elements except s_t are pure Gaussian noise. We further feed $\hat{\tau}_t^N$ into the backward process of diffusion

to generate the subsequent trajectory:

$$p_\theta(\hat{\tau}_t^{i-1} | \hat{\tau}_t^i) = \mathcal{N}(\mu_\theta(\hat{\tau}_t^i, i) + \rho \nabla \mathcal{J}_\phi(\hat{\tau}_t^i, i), \beta_i \mathbf{I}), \quad (5)$$

$$\mu_\theta(\hat{\tau}_t^i, i) = \frac{\sqrt{\alpha^i(1-\bar{\alpha}^{i-1})}}{1-\bar{\alpha}^{i-1}} \hat{\tau}_t^i + \frac{\sqrt{\bar{\alpha}^{i-1}\beta^i}}{1-\bar{\alpha}^i} \hat{\tau}_t^{i,0}. \quad (6)$$

Here $\hat{\tau}_t^{i,0} = \psi_\theta(\hat{\tau}_t^i, i)$ represents the τ_t^0 constructed from $\hat{\tau}_t^i$ at diffusion step i , $\psi_\theta(\cdot, \cdot)$ is a network for trajectory generation, $i \sim [1, N]$ is the diffusion step, ρ represents the guidance scale, $\mathcal{J}_\phi(\cdot, \cdot)$ is a learned function to predict the return given any noisy trajectory τ_t^i . We abbreviate $\hat{\tau}_t^0$ to $\hat{\tau}_t$ for convenience, $\hat{\tau}_t = \{(s_t, \hat{a}_t), (\hat{s}_{t+1}, \hat{a}_{t+1}), \dots, (\hat{s}_{t+H}, \hat{a}_{t+H})\}$. $\hat{\tau}_t$ is considered as **the subsequent trajectory** of s_t . We take out the \hat{a}_t in $\hat{\tau}$ as the action corresponding to the state s_t .

3.2. Contrastive Module

Although the Planning Module can independently generate the action responding to the environment, its performance is limited due to its plain base distribution and its neglecting of the differences among training samples. Fortunately, this can be improved via the Contrastive Module, which adopts contrastive learning to pull the states in subsequent trajectory toward the high-return states and push them away from the low-return states. Different from the previous works (Laskin et al., 2020; Qiu et al., 2022; Yuan & Lu, 2022; Agarwal et al., 2020) which apply contrastive learning to obtain a better representation, we contrast the return of states for reaching high-return states. In the following parts, we first introduce the construction of contrastive sample sets, and then we explain how we perform contrastive learning to improve the base distribution of the Planning Module.

3.2.1. SAMPLE POSITIVE AND NEGATIVE STATES

Defining positive samples and negative samples are necessary before applying contrastive learning. Intuitively, we can naively use hard thresholds to split states into positive and negative sets. However, such a radical method is unable to fully utilize samples located near the boundaries. Thus, we propose to conduct probabilistic partitioning.

Specifically, for an arbitrary state s_t in the offline dataset, we compute its return v_t first. Then, inspired by Thoma et al. (2020), we propose a soft classification mechanism to obtain the probability of a state being classified as a positive sample or a negative sample. Specifically, the probability is computed by improved influence functions:

$$p^+(s_t) \triangleq g^+(v_t) = \frac{1}{1 + e^{\sigma(\xi - v_t)}}, \quad (7)$$

$$p^-(s_t) \triangleq g^-(v_t) = \frac{1}{1 + e^{\sigma(v_t - \zeta)}}, \quad (8)$$

where $p^+(s_t)$ denotes the probability of s_t being grouped into positive samples and $p^-(s_t)$ denotes the probability of s_t being grouped into negative samples.

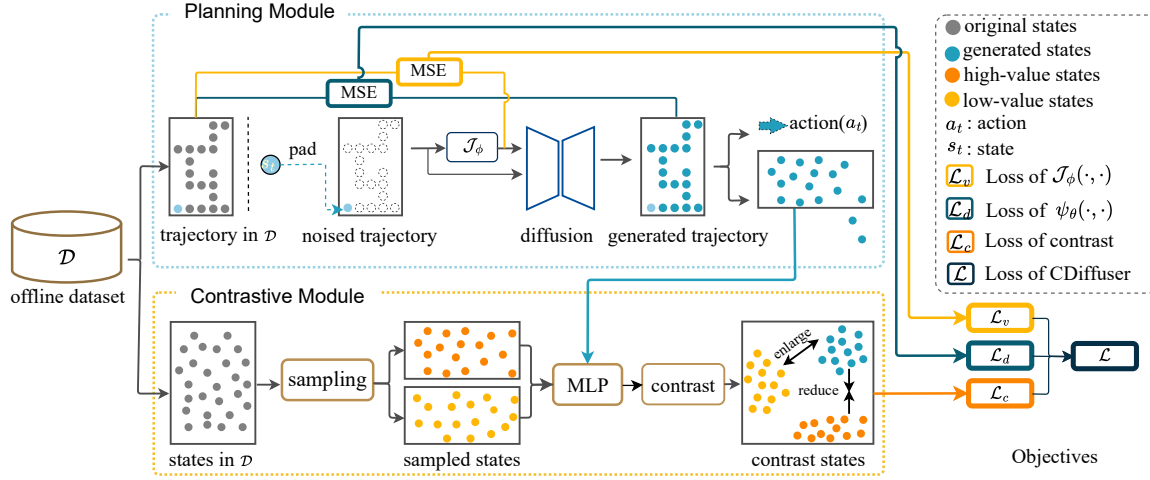


Figure 2. The overall framework of CDiffuser. CDiffuser is composed of two modules, namely the Planning Module and the Contrastive Module. The Planning Module is designed to generate the subsequent trajectories, and the Contrastive Module is designed to pull the states in the generated trajectories toward the high-return states and push them away from the low-return states during the training phase.

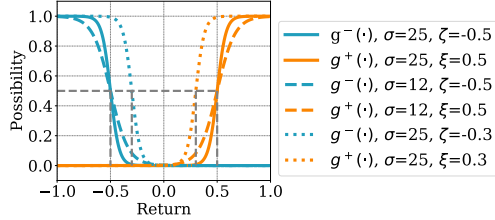


Figure 3. Improved influence functions.

In our improved influence functions, ξ and ζ are the fuzzy centers of boundaries for positive and negative samples respectively, σ represents the fuzzy coefficient. As is shown in Figure 3, with ξ getting larger, fewer samples are grouped into positive samples. With ζ getting smaller, fewer samples are grouped into negative samples. A larger σ makes $g^+(v_t)$ and $g^-(v_t)$ sharper.

3.2.2. CONSTRAIN THE TRAJECTORY WITH CONTRASTIVE LEARNING

To constrain the states in subsequent trajectories while avoiding the cost of running the whole backward denoising process, we leverage the noised trajectory in the diffusion backward process to reconstruct a neat trajectory, *i.e.*, $\hat{\tau}_t^{i,0} = \{(\hat{s}_t^{i,0}, \hat{a}_t^{i,0}), (\hat{s}_{t+1}^{i,0}, \hat{a}_{t+1}^{i,0}), \dots, (\hat{s}_{t+H}^{i,0}, \hat{a}_{t+H}^{i,0})\}$ from τ_t^i for any arbitrary diffusion step i . Then, we extract states in $\hat{\tau}_t^{i,0}$ as $\mathcal{S}_{\hat{\tau}_t^{i,0}} = \{\hat{s}_{t+1}^{i,0}, \hat{s}_{t+2}^{i,0}, \dots, \hat{s}_{t+H}^{i,0}\}$. For each state $\hat{s}_h^{i,0} \in \mathcal{S}_{\hat{\tau}_t^{i,0}}$, we sample κ states via Equation (7) as positive samples and κ states via Equation (8) as negative samples from the offline dataset. These samples form a positive sample set \mathcal{S}_h^+ and a negative sample set \mathcal{S}_h^- respectively.

Inspired by Schroff et al. (2015) and Sohn (2016), to apply contrastive learning to the scenario of multiple positive samples and impose aggressive constraints, we removed the positive sample term from the denominator polynomial in Equation (2) and propose the following equation to pull

the states in the generated subsequent trajectory toward the high-return states and away from the low-return states:

$$\mathcal{L}_h^i = -\log \frac{\sum_{k=0}^{\kappa} \exp(\text{sim}(f(\hat{s}_h^{i,0}), f(\mathcal{S}_h^+))/T)}{\sum_{k=0}^{\kappa} \exp(\text{sim}(f(\hat{s}_h^{i,0}), f(\mathcal{S}_h^-))/T)}, \quad (9)$$

where $\mathcal{S}_h^+ \in \mathcal{S}_h^+$, $\mathcal{S}_h^- \in \mathcal{S}_h^-$. $f(\cdot)$ represents the projection function, T represents the temperature, and $\text{sim}(\cdot, \cdot)$ denotes the cosine similarity, which is computed as

$$\text{sim}(\mathbf{a}, \mathbf{b}) = \frac{\mathbf{a}^\top \mathbf{b}}{\|\mathbf{a}\| \cdot \|\mathbf{b}\|}. \quad (10)$$

3.3. Model Learning

Recall that the action responding to state s_t is one of the elements in the generated trajectory, and is influenced by the return predictor $\mathcal{J}_\phi(\cdot, \cdot)$ and contrastive learning. Therefore, we optimize our method from the perspective of trajectory generation, return prediction, and trajectory generation constrain.

Specifically, we optimize the trajectory generation by minimizing the Mean Square Error between the ground truth and neat trajectory predicted by $\psi_\theta(\cdot, \cdot)$ given any intermediate noisy trajectories as input:

$$\mathcal{L}_d = \mathbb{E}_{\tau_t \in \mathcal{D}, t > 0, i \sim [1, N]} [\|\tau_t - \psi_\theta(\tau_t^i, i)\|^2], \quad (11)$$

where i denotes the step of diffusion, τ_t^i is obtained in the i -th step of forward process.

We optimize the return predictor by minimizing the Mean Square Error between the predicted return $\mathcal{J}_\phi(\tau_t^i, i)$ and the ground-truth return v_t :

$$\mathcal{L}_v = \mathbb{E}_{\tau_t \in \mathcal{D}, t > 0, i \sim [1, N]} [\|\mathcal{J}_\phi(\tau_t^i, i) - v_t\|^2]. \quad (12)$$

Table 1. The average normalized score of different methods on various environments, with \pm denoting the standard deviation. The mean and standard deviation are computed over 10 random seeds. The best and the second-best results of each setting are marked as **bold** and underline, respectively.

Dataset	Environment	CQL	IQL	DT	TT	MOPO	Diffuser	DD	CDiffuser
Med-Expert	HalfCheetah	91.6	86.7	86.8	95.0	63.3	88.9	90.6	<u>92.0</u> \pm 0.4
Med-Expert	Hopper	105.4	91.5	107.6	110.0	23.7	103.3	<u>111.8</u>	112.4 \pm 1.2
Med-Expert	Walker2d	<u>108.8</u>	109.6	108.1	101.9	44.6	106.9	<u>108.8</u>	108.2 \pm 0.4
Medium	HalfCheetah	44.0	<u>47.4</u>	42.6	46.9	42.3	42.8	49.1	43.9 \pm 0.9
Medium	Hopper	58.5	66.3	67.6	61.1	28.0	74.3	<u>79.3</u>	92.3 \pm 2.6
Medium	Walker2d	72.5	78.3	74.0	79.0	17.8	79.6	<u>82.5</u>	82.9 \pm 0.5
Med-Replay	HalfCheetah	<u>45.5</u>	44.2	36.6	41.9	53.1	37.7	39.3	40.0 \pm 1.1
Med-Replay	Hopper	95	94.7	82.7	91.5	67.5	93.6	100	<u>96.4</u> \pm 1.1
Med-Replay	Walker2d	77.2	73.9	66.6	<u>82.6</u>	39.0	70.6	75	84.2 \pm 1.2
U-Maze	Maze2d	5.7	47.4	-	-	-	<u>113.9</u>	0.0	142.9 \pm 2.2
Medium	Maze2d	5.0	34.9	-	-	-	<u>121.5</u>	0.0	140.0 \pm 0.7
Large	Maze2d	12.5	58.6	-	-	-	<u>123.0</u>	0.0	131.5 \pm 3.2
Mixed	Kitchen	52.4	51.0	-	-	-	42.5	<u>65.0</u>	65.0 \pm 1.3
Partial	Kitchen	51.2	46.3	-	-	-	40.0	<u>57.0</u>	58.0 \pm 1.9

We constrain the trajectory generation with a weighted contrastive loss:

$$\mathcal{L}_c = \mathbb{E}_{t>0, i \sim [1, N]} \left[\sum_{h=t}^{t+H} \frac{1}{h+1} \mathcal{L}_h^i \right], \quad (13)$$

in which the coefficient $\frac{1}{h+1}$ decreases as h increases since the importance gradually diminishes as it approaches the end of the planning horizon.

Hence, the overall objective function of CDiffuser can be written as a weighted sum of the aforementioned loss terms:

$$\mathcal{L} = \lambda_d \mathcal{L}_d + \lambda_v \mathcal{L}_v + \lambda_c \mathcal{L}_c, \quad (14)$$

where $\lambda_d, \lambda_v, \lambda_c$ are hyperparameters, which balance the importances of the corresponding learning targets¹. The pseudo code of CDiffuser is presented in Appendix A.1, and the detail of implementation will be discussed in the next section.

4. Experiments

In this section, we evaluate the performance of CDiffuser in three locomotion environments under three settings, as well as complex tasks including a navigation environment Maze2d under three settings and a high-dimensional operation environment Kitchen under two settings.

4.1. Experiment Settings

Environments and datasets. We evaluate the performance of CDiffuser on the locomotion tasks, navigation tasks and operation tasks. Specifically, we evaluate the locomotion

¹Please notice that the return predictor $\mathcal{J}\phi(\cdot, \cdot)$ and $\psi_\theta(\cdot, \cdot)$ are independent, thus optimizing $\mathcal{J}\phi(\cdot, \cdot)$ and $\psi_\theta(\cdot, \cdot)$ with \mathcal{L} is identical to separately optimizing $\mathcal{J}\phi(\cdot, \cdot)$ with \mathcal{L}_v and $\psi_\theta(\cdot, \cdot)$ with \mathcal{L}_d and \mathcal{L}_c . Please refer to Appendix A.5 for details.

capability of CDiffuser on Halfcheetah, Hopper, Walker2d, evaluate the navigation capability of CDiffuser on Maze2d, and evaluate the ability of CDiffuser in complex tasks on Kitchen. For each environment, we train CDiffuser with various scales of offline datasets provided by D4RL (Fu et al., 2020), and test the performance of CDiffuser on the corresponding environments.

Baselines. We compare CDiffuser with diffusion-free methods such as CQL (Kumar et al., 2020), IQL (Kostrikov et al., 2021), MOPO (Yu et al., 2020), Decision Transformer (DT) (Chen et al., 2021) and Trajectory Transformer (TT) (Janner et al., 2021). Further, we compare CDiffuser with diffusion-based methods Diffuser (Janner et al., 2022) and Decision Diffuser (DD) (Ajay et al., 2023), which apply diffusion to model RL as sequence generation problems.

Implementation details. We adopt U-Net (Ronneberger et al., 2015) as the denoise network $\psi_\theta(\cdot, \cdot)$ and the return predictor $\mathcal{J}\phi(\cdot, \cdot)$, and adopt a linear layer with *Sigmoid* as the activation function as the projector $f(\cdot)$. Our model is trained on a device with 4 NVIDIA A40 GPUs (48GB GPU memory, 37.4 TFLOPS computing capabilities), Intel Gold 5220 CPU (72 cores, 2.20GHz clock frequency) and 504G memory, optimized by Adam (Kingma & Ba, 2014) optimizer. Details of hyper-parameters are shown in Appendix A.3.

4.2. Benchmark Results

We compare CDiffuser to baseline methods with respect to the normalized average returns (Fu et al., 2020) obtained during online evaluation. We conducted 10 trials with different seeds and reported the average results. The results of CDiffuser and baseline methods are summarized in Table 1.

From Table 1, we can observe that: (1) Compared with all the baseline methods, CDiffuser achieves the best or the second-best performance on 6 out of 9 locomotion tasks and achieves the best performance on all the two high-

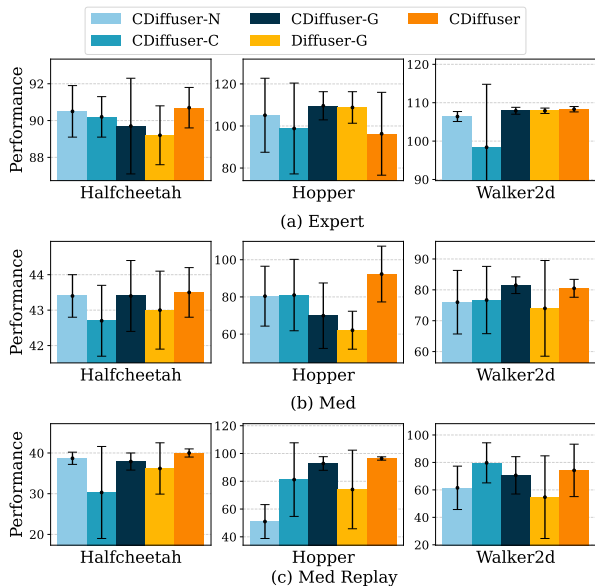


Figure 4. Results of the ablation experiments on different variants.

dimensional operation tasks, demonstrating the outstanding performance of CDiffuser under periodic settings. Moreover, CDiffuser achieves the best performance on all the three navigation tasks, demonstrating the excellent ability of CDiffuser in long-term planning. When it comes to the Kitchen environment, CDiffuser outperforms all the baselines on 2 out of 2 tasks, demonstrating the ability of CDiffuser in complex tasks. (2) Compared with our backbone method Diffuser, CDiffuser outperforms Diffuser in all the 14 tasks, which demonstrates the effectiveness of contrast in boosting diffusion-based RL methods. Moreover, CDiffuser exhibits more improvement in Med and Med-Replay datasets than the Med-Expert datasets. Since Med-Expert datasets have more high-return samples, it is easier for Diffuser to learn and achieve better results. However, both Med and Med-Replay have more low-return samples, which increases the difficulty for Diffuser to learn a good policy. These results demonstrate that CDiffuser is more effective on datasets with many low-return samples, such as Med and Med-Replay.

4.3. Ablation Studies

We conduct ablation studies to further investigate the impact of our contrastive mechanism on performance. Specifically, we explore the following four variants:

- **CDiffuser-N**: only apply the samples with high-return to train the model.
- **CDiffuser-C**: remove contrastive learning from CDiffuser, *i.e.*, remove \mathcal{L}_c from Equation (14).
- **CDiffuser-G**: remove the guidance from CDiffuser, *i.e.*, removing $\rho \nabla \mathcal{J}_\phi(\cdot, \cdot)$ from Equation (5).
- **Diffuser-G**: remove the classifier guidance from Diffuser.

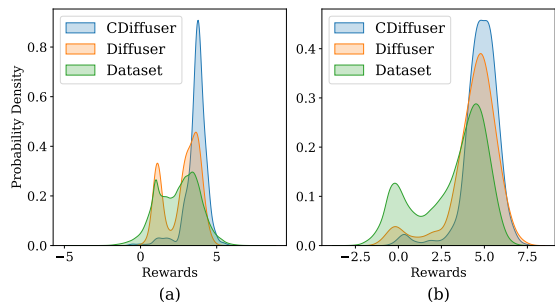


Figure 5. Distribution of rewards from dataset and from the base distribution of Diffuser and CDiffuser on Walker2d-Med-Replay (a) and Halfcheetah-Med-Replay (b). The base distribution of Diffuser expresses a higher similarity to the dataset distribution, while CDiffuser concentrates more on the high reward area.

The results are summarized in Figure 4, from which we can conclude the following key findings: (1) **Improving the base distribution benefits the performance.** CDiffuser-G outperforms Diffuser-G in 8 out of 9 tasks. Given that both CDiffuser-G and Diffuser-G eliminate guidance and generate trajectories with their base distributions, this suggests the base distribution of CDiffuser-G leads an improved performance, *i.e.*, improving the base distribution is beneficial. (2) **The contrastive mechanism benefits the performance.** CDiffuser-C, which eliminates the contrastive mechanism from CDiffuser, exhibits poorer performance across all nine tasks than CDiffuser. This suggests that the contrastive mechanism indeed provides benefits. (3) **Applying only the high-return samples in training diminishes benefits in some cases.** Compared with CDiffuser, CDiffuser-N is trained solely with high-value samples. Surprisingly, it achieves a lower performance than CDiffuser in all of 9 tasks, indicating that relying exclusively on high-return samples brings minimal benefits.

4.4. Further Investigation

To further investigate the performance of CDiffuser, we analyze the CDiffuser’s base distribution, state-reward distribution and plan-execution consistency.

Base distribution analysis. Recall that we improve the base distribution of diffusion model with contrastive learning to enhance the performance. To assess the improvements introduced by CDiffuser on the base distribution, selecting Walker2d-Med-Replay and Halfcheetah-Med-Replay as representative datasets, we iteratively randomly sample trajectories using the base distribution of Diffuser and CDiffuser without guidance. Then we extract the actions in the trajectories, interact with the environment, and record the rewards provided by the environment. We further present the rewards probability density of Diffuser, CDiffuser and dataset in Figure 5. It can be observed that, on both Walker2d-Med-Replay and Halfcheetah-Med-Replay, Diffuser shares a similar pattern with dataset in rewards probability density, which corresponds to our claim in Section 1, namely

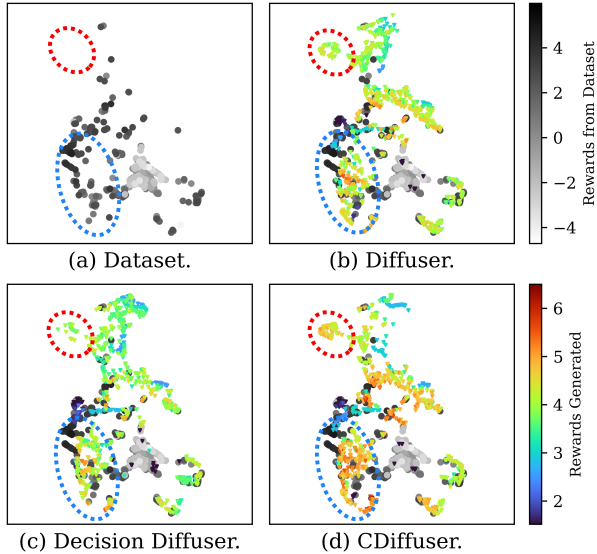


Figure 6. The distribution of state and reward. It is better to view in color mode. CDiffuser achieves higher rewards in both in-distribution areas (circled with blue) and out-of-distribution areas (circled with red).

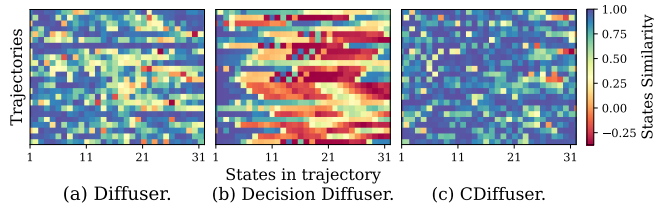


Figure 7. The similarities between the states in the generated trajectories and actual states. The generated states of CDiffuser are more similar with the actual states, demonstrating the better long-term dynamic consistency.

that the plain base distribution of Diffuser stays close to the dataset distribution. However, the rewards probability density of CDiffuser concentrates more on the high-reward area, which intuitively illustrates that the base distribution is enhanced by our contrastive learning mechanism. As a result, CDiffuser performs better than Diffuser.

State-reward distribution analysis. To investigate the states explored by CDiffuser, we randomly collect the (state, reward) pairs from the offline dataset of Walker2d-Med-Replay and the (state, reward) pairs collected when Diffuser, Decision Diffuser, and CDiffuser interact with the environment. Here, we choose Diffuser and Decision Diffuser as both of them apply diffusion to model RL as a sequence generation problem. We compare the results in Figure 6. In Figure 6, each scatter represents a state mapped by UMAP (McInnes et al., 2018), and its color denotes the reward gained in the corresponding state. From the results illustrated in Figure 6, we can observe that: in both in-distribution states (circled with blue) and out-of-distribution states (circled with red), CDiffuser gains higher rewards, demonstrating the ability of CDiffuser in generating state-action pairs with higher rewards.

Table 2. The improvements of the normalized score after transplanting the contrastive mechanism of CDiffuser to Decision Diffuser (DD⁺) and Diffuser (Diffuser⁺), with \pm denoting the variance.

Dataset	Environment	DD ⁺	Diffuser ⁺
Med-Expert	Halfcheetah	0	3.1 \pm 0.4
Med-Expert	Hopper	5.4 \pm 1.2	9.1 \pm 1.2
Med-Expert	Walker2d	6.5 \pm 0.9	1.3 \pm 0.4

Plan-execution consistency analysis. We use the plan-execution consistency to denote the similarity between the states in the planned trajectory and the states encountered by the agent during its interaction with the environment. It reflects the models’ capability in modeling the environment. To investigate the plan-execution consistency of CDiffuser, we randomly take 24 trajectories generated by Diffuser, Decision Diffuser, and CDiffuser. For each generated trajectory, we take the states of consecutive 32 steps and compute the similarity between each generated state and the actual state of the same step provided by the environment. Thus, there are 24×32 similarity values for each model, which corresponds to a similarity matrix as the subgraphs in Figure 7 illustrated. Each line in the subgraphs of Figure 7 represents a generated trajectory, and the grids of each line represent the similarity of the states in the generated trajectory and the states provided by the environment. From Figure 7, we can observe that: (1) Most grids in Figure 7 (c) are blue, which denotes that most generated states are consistent with the actual states; (2) Figure 7 (c) contains more blue grids than Figure 7 (a) and (b), which denotes that CDiffuser has better plan-execution consistency than Diffuser and Decision Diffuser. Since the difference between CDiffuser and Diffuser is the contrastive module, combining Figure 6 and Figure 7, we can conclude that the contrastive module benefits the plan-execution consistency of CDiffuser and makes CDiffuser gain high rewards in both in-distribution and out-of-distribution situations.

4.5. Compatibility Study

Recall that we design the contrastive mechanism to improve the unguided distribution for better performance. This mechanism can be easily transplanted onto other diffusion-based methods, such as Decision Diffuser (Ajay et al., 2023). We transplant the contrastive mechanism of CDiffuser to Decision Diffuser, evaluate and compare the improvement on three environments. The improvements are summarized in Table 2, in which DD⁺ and Diffuser⁺ denote the improvement of introducing contrast mechanism in Decision Diffuser and Diffuser correspondingly. As we can observe, DD⁺ achieves noticeable improvement in 2 out of 3 tasks and Diffuser⁺ gains improvement in 3 out of 3 tasks, which demonstrates the portability of the contrast mechanism of CDiffuser. Interestingly, DD⁺ is unable to achieve any improvement in Halfcheetah-Med-Expert. This could be attributed to the separated training (sampling) of states and actions in Decision Diffuser, which results in a failure to

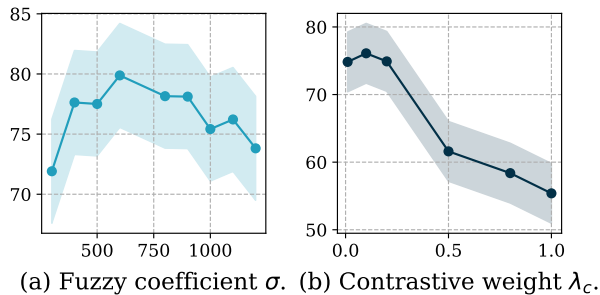


Figure 8. The impact of hyperparameters.

effectively model their joint distribution.

4.6. Hyperparameter Analysis

The contrastive mechanism applied in this paper is significantly influenced by two factors: the selection of positive samples and negative samples, and the weight of contrastive loss, which are controlled by hyperparameter σ and λ_c respectively. To investigate the impact of σ and λ_c on the performance, we conduct the hyperparameter study. In the experiment, all the settings remain the same except the value of the tested hyper-parameter. The results are illustrated in Figure 8. It can be observed that: (1) With the increase of σ , the performance gradually increases and then decreases. The reason is that, σ provides the tolerance for distinguishing between positive and negative samples in classification. Moreover, a σ that is too low blurs the boundary between positive and negative samples, while a σ that is too high sharpens the boundary. Both scenarios lead to unsatisfactory performance. (2) With the increase of λ_c , the performance increases at the very beginning steps but decreases then. λ_c balance generating high value states and generating samples that conform to the joint distribution of the current state and possible future states. However, over-emphasizing the contrast will lead to neglecting the dataset distribution, thus relinquishing the generalization of diffusion and resulting in a decrease in performance.

5. Related Works

5.1. Diffusion in Decision Making

We group the diffusion-based methods in RL into action generation methods and trajectory generation methods. The action generation methods (Ada et al., 2023; Wang et al., 2022; Chen et al., 2022; Chi et al., 2023) adopt diffusion models as policies to predict the action of the current step. One of the typical works in this group is Diffusion Q-learning (Wang et al., 2022), which proposes to design the policy as a diffusion model and improve it with double Q-learning architecture. Following Diffusion Q-Learning, SRDPs (Ada et al., 2023) incorporates state reconstruction feature learning into the recent category of diffusion policies to address the out-of-distribution generalization problem. The second group of methods generate the subsequent trajectory including the action to take at the current step by diffusion. For in-

stance, Diffuser (Janner et al., 2022) models trajectories as sequences of state-action pairs. Based on Diffuser, Decision Diffuser (Ajay et al., 2023) proposes to predict state sequences with a diffusion model conditioned on historical information, and adopts a reverse dynamic model to predict actions based on the generated state sequence. Though these methods have gain significant achievements, they neglect the differences of high-return samples and low-return samples and are limited by their plain base distribution.

5.2. Contrastive Learning in RL

The motivation for introducing contrastive learning in RL is to enrich the representation in the previous works. We group these works into three types. The first type of methods apply contrastive learning to enhance the state representations (Laskin et al., 2020; Qiu et al., 2022). For instance, Laskin et al. (2020) propose to learn image representations via contrastive learning; Qiu et al. (2022) propose to learn the transition with contrastive learning. The second type of methods apply contrastive learning to learn the representations of tasks. For instance, Yuan & Lu (2022) apply contrastive learning to enhance the representation of tuples to distinguish between different tasks; Agarwal et al. (2020) apply contrastive learning to learn the representations of the environments. Some works apply contrastive learning in other ways. For instance, Laskin et al. (2022) utilizes contrastive learning to learn behavior representations and maximizes the entropy to encourage behavioral diversity. In contrast to the methods mentioned above, CDiffuser adopts contrastive learning to constrain the generated sample, rather than learning representations.

6. Conclusion and Discussion

In this paper, we introduce CDiffuser for offline RL, which improves the base distribution by introducing contrastive learning. Different from the previous works which apply contrastive learning to enhance the representation, we perform contrastive learning over the return of states. Specifically, we apply diffusion to generate the subsequent trajectory for planning, and constrain the states in the generated trajectory toward the states with high returns and away from the states with low returns to improve the base distribution. In that way, the actions taken by the agent are always toward the high-return states, which makes the agent gain better performance in the online evaluation. We evaluated CDiffuser on 14 D4RL benchmarks, the results demonstrate that our CDiffuser achieves outstanding performance. The ablation studies and investigations further substantiated the rationality of CDiffuser. We currently focus on performing contrastive learning over the return of states to enhance the base distribution in this paper. Yet, this contrastive mechanism can also be applied to other levels, such as action or state-action pairs, or even at the latent of trajectories. We will leave it to future works.

References

- Ada, S. E., Oztop, E., and Ugur, E. Diffusion policies for out-of-distribution generalization in offline reinforcement learning. *arXiv preprint arXiv:2307.04726*, 2023.
- Agarwal, R., Machado, M. C., Castro, P. S., and Bellemare, M. G. Contrastive behavioral similarity embeddings for generalization in reinforcement learning. In *International Conference on Learning Representations*, 2020.
- Ajay, A., Du, Y., Gupta, A., Tenenbaum, J. B., Jaakkola, T. S., and Agrawal, P. Is conditional generative modeling all you need for decision making? In *The Eleventh International Conference on Learning Representations*, 2023. URL <https://openreview.net/forum?id=sP1fo2K9DFG>.
- Chen, H., Lu, C., Ying, C., Su, H., and Zhu, J. Offline reinforcement learning via high-fidelity generative behavior modeling. *arXiv preprint arXiv:2209.14548*, 2022.
- Chen, H., Lu, C., Wang, Z., Su, H., and Zhu, J. Score regularized policy optimization through diffusion behavior. *arXiv preprint arXiv:2310.07297*, 2023.
- Chen, L., Lu, K., Rajeswaran, A., Lee, K., Grover, A., Laskin, M., Abbeel, P., Srinivas, A., and Mordatch, I. Decision transformer: Reinforcement learning via sequence modeling. *Advances in neural information processing systems*, 34:15084–15097, 2021.
- Chi, C., Feng, S., Du, Y., Xu, Z., Cousineau, E., Burchfiel, B., and Song, S. Diffusion policy: Visuomotor policy learning via action diffusion. *arXiv preprint arXiv:2303.04137*, 2023.
- Dhariwal, P. and Nichol, A. Q. Diffusion models beat GANs on image synthesis. In Beygelzimer, A., Dauphin, Y., Liang, P., and Vaughan, J. W. (eds.), *Advances in Neural Information Processing Systems*, 2021. URL <https://openreview.net/forum?id=AAWuCVzaVt>.
- Fatemi, M., Wu, M., Petch, J., Nelson, W., Connolly, S. J., Benz, A., Carnicelli, A., and Ghassemi, M. Semi-markov offline reinforcement learning for healthcare. In *Conference on Health, Inference, and Learning*, pp. 119–137. PMLR, 2022.
- Feller, W. On the theory of stochastic processes, with particular reference to applications. 1949. URL <https://api.semanticscholar.org/CorpusID:121027442>.
- Fu, J., Kumar, A., Nachum, O., Tucker, G., and Levine, S. D4rl: Datasets for deep data-driven reinforcement learning. *arXiv preprint arXiv:2004.07219*, 2020.
- Ho, J., Jain, A., and Abbeel, P. Denoising diffusion probabilistic models. *Advances in Neural Information Processing Systems*, 33:6840–6851, 2020.
- Janner, M., Li, Q., and Levine, S. Offline reinforcement learning as one big sequence modeling problem. *Advances in neural information processing systems*, 34:1273–1286, 2021.
- Janner, M., Du, Y., Tenenbaum, J., and Levine, S. Planning with diffusion for flexible behavior synthesis. In *International Conference on Machine Learning*, pp. 9902–9915. PMLR, 2022.
- Jaques, N., Shen, J. H., Ghandeharioun, A., Ferguson, C., Lapedriza, A., Jones, N., Gu, S., and Picard, R. Human-centric dialog training via offline reinforcement learning. In *Proceedings of the 2020 Conference on Empirical Methods in Natural Language Processing (EMNLP)*, pp. 3985–4003, 2020.
- Khosla, P., Teterwak, P., Wang, C., Sarna, A., Tian, Y., Isola, P., Maschinot, A., Liu, C., and Krishnan, D. Supervised contrastive learning. *Advances in neural information processing systems*, 33:18661–18673, 2020.
- Kingma, D. P. and Ba, J. Adam: A method for stochastic optimization. *arXiv preprint arXiv:1412.6980*, 2014.
- Kostrikov, I., Fergus, R., Tompson, J., and Nachum, O. Offline reinforcement learning with fisher divergence critic regularization. In *International Conference on Machine Learning*, pp. 5774–5783. PMLR, 2021.
- Kumar, A., Zhou, A., Tucker, G., and Levine, S. Conservative q-learning for offline reinforcement learning. *Advances in Neural Information Processing Systems*, 33:1179–1191, 2020.
- Laskin, M., Srinivas, A., and Abbeel, P. Curl: Contrastive unsupervised representations for reinforcement learning. In *International Conference on Machine Learning*, pp. 5639–5650. PMLR, 2020.
- Laskin, M., Liu, H., Peng, X. B., Yarats, D., Rajeswaran, A., and Abbeel, P. Unsupervised reinforcement learning with contrastive intrinsic control. *Advances in Neural Information Processing Systems*, 35:34478–34491, 2022.
- Levine, S., Kumar, A., Tucker, G., and Fu, J. Offline reinforcement learning: Tutorial, review, and perspectives on open problems. *arXiv preprint arXiv:2005.01643*, 2020.
- McInnes, L., Healy, J., Saul, N., and Großberger, L. Umap: Uniform manifold approximation and projection. *Journal of Open Source Software*, 3(29), 2018.

- Oord, A. v. d., Li, Y., and Vinyals, O. Representation learning with contrastive predictive coding. *arXiv preprint arXiv:1807.03748*, 2018.
- Prudencio, R. F., Maximo, M. R., and Colombini, E. L. A survey on offline reinforcement learning: Taxonomy, review, and open problems. *IEEE Transactions on Neural Networks and Learning Systems*, 2023.
- Qiu, S., Wang, L., Bai, C., Yang, Z., and Wang, Z. Contrastive ucbl: Provably efficient contrastive self-supervised learning in online reinforcement learning. In *International Conference on Machine Learning*, pp. 18168–18210. PMLR, 2022.
- Ronneberger, O., Fischer, P., and Brox, T. U-net: Convolutional networks for biomedical image segmentation. In *Medical Image Computing and Computer-Assisted Intervention—MICCAI 2015: 18th International Conference, Munich, Germany, October 5-9, 2015, Proceedings, Part III 18*, pp. 234–241. Springer, 2015.
- Schroff, F., Kalenichenko, D., and Philbin, J. Facenet: A unified embedding for face recognition and clustering. In *Proceedings of the IEEE conference on computer vision and pattern recognition*, pp. 815–823, 2015.
- Shi, T., Chen, D., Chen, K., and Li, Z. Offline reinforcement learning for autonomous driving with safety and exploration enhancement. *arXiv preprint arXiv:2110.07067*, 2021.
- Sohl-Dickstein, J., Weiss, E., Maheswaranathan, N., and Ganguli, S. Deep unsupervised learning using nonequilibrium thermodynamics. In *International conference on machine learning*, pp. 2256–2265. PMLR, 2015.
- Sohn, K. Improved deep metric learning with multi-class n-pair loss objective. *Advances in neural information processing systems*, 29, 2016.
- Song, J., Meng, C., and Ermon, S. Denoising diffusion implicit models. In *International Conference on Learning Representations*.
- Song, J., Meng, C., and Ermon, S. Denoising diffusion implicit models. In *International Conference on Learning Representations*, 2020.
- Sutton, R. S. and Barto, A. G. *Reinforcement learning: An introduction*. MIT press, 2018.
- Thoma, J., Paudel, D. P., and Gool, L. V. Soft contrastive learning for visual localization. *Advances in Neural Information Processing Systems*, 33:11119–11130, 2020.
- Wang, Z., Hunt, J. J., and Zhou, M. Diffusion policies as an expressive policy class for offline reinforcement learning. In *The Eleventh International Conference on Learning Representations*, 2022.
- Xiao, T. and Wang, D. A general offline reinforcement learning framework for interactive recommendation. In *Proceedings of the AAAI Conference on Artificial Intelligence*, volume 35, pp. 4512–4520, 2021.
- Yeh, C.-H., Hong, C.-Y., Hsu, Y.-C., Liu, T.-L., Chen, Y., and LeCun, Y. Decoupled contrastive learning. In *European Conference on Computer Vision*, pp. 668–684. Springer, 2022.
- Yu, T., Thomas, G., Yu, L., Ermon, S., Zou, J. Y., Levine, S., Finn, C., and Ma, T. Mopo: Model-based offline policy optimization. *Advances in Neural Information Processing Systems*, 33:14129–14142, 2020.
- Yuan, H. and Lu, Z. Robust task representations for offline meta-reinforcement learning via contrastive learning. In *International Conference on Machine Learning*, pp. 25747–25759. PMLR, 2022.
- Yue, Y., Kang, B., Ma, X., Xu, Z., Huang, G., and Yan, S. Boosting offline reinforcement learning via data rebalancing. *arXiv preprint arXiv:2210.09241*, 2022.

A. Appendix

A.1. Pseudocode of CDiffuser.

Algorithm 1 Training

- 1: Calculate the candidate set \mathcal{C} .
 - 2: **while** not converged **do**
 - 3: $\tau_t, v_t \sim \mathcal{D}$.
 - 4: $i \sim [1, N]$.
 - 5: Generate τ_t^i .
 - 6: Reconstruct τ_t as $\hat{\tau}_t^{i,0} = \psi_\theta(\tau_t^i, i)$.
 - 7: Calculate loss \mathcal{L}_d with Equation (11).
 - 8: Calculate loss \mathcal{L}_v with Equation (12).
 - 9: Extract STATES in $\hat{\tau}_t^{i,0}$ as $\mathcal{S}_{\hat{\tau}_t^{i,0}} = \{\hat{s}_{t+1}^{i,0}, \hat{s}_{t+2}^{i,0}, \dots, \hat{s}_{t+H}^{i,0}\}$.
 - 10: **for** $\hat{s}_h^{i,0}$ in $\mathcal{S}_{\hat{\tau}_t^{i,0}}$ **do**
 - 11: Sample \mathcal{S}^+ and \mathcal{S}^- with Equation (7) and Equation (8).
 - 12: Calculate \mathcal{L}_h^i using Equation (9).
 - 13: **end for**
 - 14: Calculate \mathcal{L}_c using Equation (13).
 - 15: Calculate \mathcal{L} using Equation (14).
 - 16: Update model by taking gradient decent with \mathcal{L} .
 - 17: **end while**
-

Algorithm 2 Planning

- Require:** CDiffuser $\psi_\theta(\cdot, \cdot)$, return-to-go predictor $\mathcal{J}_\phi(\cdot, \cdot)$, guidance scale ρ , co-variances Σ^i .
- 1: $t \leftarrow 1$.
 - 2: **while** not done **do**
 - 3: Observe STATE s_t ; sample $\tau_t^N \sim \mathcal{N}(\mathbf{0}, \mathbf{I})$
 - 4: **for** $i = N, N-1, \dots, 1$ **do**
 - 5: Predict return-to-go with $\mathcal{J}_\phi(\hat{\tau}_t^i, i)$.
 - 6: Sample $\hat{\tau}_t^{i-1}$ using Equation (5).
 - 7: **end for**
 - 8: Extract \hat{a}_t form $\hat{\tau}^0$.
 - 9: Interact with environment using action \hat{a}_t .
 - 10: $t \leftarrow t + 1$.
 - 11: **end while**
-

A.2. Impact of hyperparameters on training stability.

To evaluate the impact of hyperparameters on training stability, we visualize the training curves of Hopper-Medium with various values of hyperparameters ξ , ζ , σ and λ_c , as is shown in Figure 9. It can be concluded that in most of situations, these hyperparameters will not unstable the training process, for example, whatever value ξ , ζ , σ and λ_c take, the training process is stable and CDiffuser converges to a certain point.

A.3. Hyper-parameters.

We consider the following hyper-parameter for CDiffuser: Learnign rate, positive bound (ξ), negative bound (ζ), fuzzy coefficient (σ), loss weight of plannign module (λ_d), loss weight of contrastive learning (λ_c), loss weight of return predictor $\mathcal{J}_\phi(\cdot, \cdot)$ (λ_v), guidance scale (ρ), diffusion steps (N) and the length of subsequent trajectory (H). Please notice that both the Planning Module and Ccntrastive Module are trained 1×10^6 steps, while the return predictor $\mathcal{J}_\phi(\cdot, \cdot)$ is trained 2×10^5 steps. Detailed hyper-parameter settings for each dataset is provided in Table 3. Following Diffuser, we perform un-guided sampling for Maze2d environments.

A.4. Visualization of positive and negative samples.

We randomly sample a subset of positive samples (states with high returns) and negative samples (states with low returns), as is shown in Figure 10. It can be observed that an agent in a STATE corresponding to a high return tends to be in a position more conducive to walking or running, such as standing upright; correspondingly, an agent with a STATE corresponding to a low return will be in a position that is hard to walk, such as having already fallen down or about to fall down. This is reasonable, since poses such as standing upright are more conducive to walking or running, which causes the agent to continue moving and results in a higher return, while poses such as having fallen or about to fall cause the environment to give a stop signal, which results in a lower return.

A.5. Optimizing $\mathcal{J}_\phi(\cdot, \cdot)$ with Equation (14)

Suppose we have the diffuison model $\psi_\theta(\cdot)$ parameterized by θ , and the return predictor \mathcal{J}_ϕ parameterized by ϕ . Following Equation (14), we have

$$\mathcal{L} = \lambda_d \mathcal{L}_d + \lambda_v \mathcal{L}_v + \lambda_c \mathcal{L}_c. \quad (15)$$

Further,

$$\mathcal{L}_d = \mathbb{E}_{\tau_t \in \mathcal{D}, t > 0, i \sim [1, N]} [\|\tau_t - \psi_\theta(\tau_t^i, i)\|^2], \quad (16)$$

$$\mathcal{L}_v = \mathbb{E}_{\tau_t \in \mathcal{D}, t > 0, i \sim [1, N]} [\|\mathcal{J}_\phi(\tau_t^i, i) - v_t\|^2]. \quad (17)$$

The training process can be viewed as a procedure of calculating gradients of all the parameters and updating them, specifically,

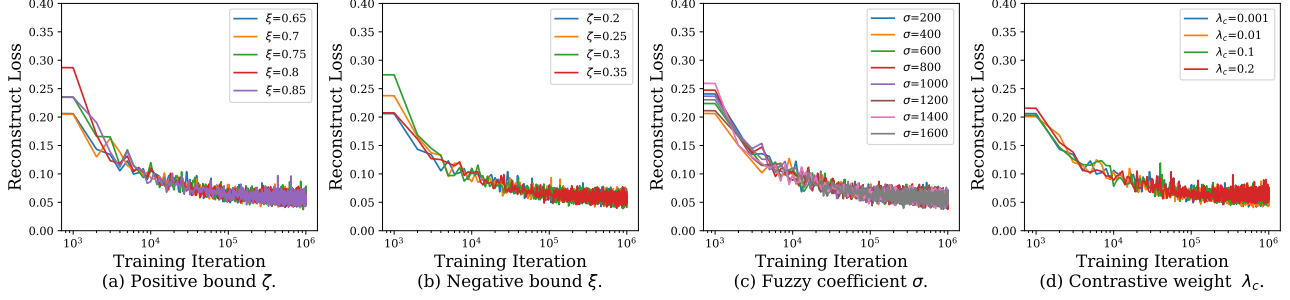

 Figure 9. Training curves of Hopper-Med with various values of ξ , ζ , σ and λ_c .

Table 3. Hyper-parameter settings for each dataset.

Dataset	Environment	learning rate	ξ	ζ	σ	λ_d	λ_v	λ_c	ρ	N	H
Med-Expert	HalfCheetah	2×10^{-4}	0.65	0.05	1.6×10^3	1	1	0.1	0.001	20	4
Med-Expert	Hopper	2×10^{-4}	0.65	0.35	1.4×10^3	1	1	0.001	0.0001	20	32
Med-Expert	Walker2d	2×10^{-4}	0.65	0.1	1×10^8	1	1	0.001	0.1	20	32
Medium	HalfCheetah	2×10^{-4}	0.85	0.2	7×10^2	1	1	0.01	0.001	20	4
Medium	Hopper	2×10^{-4}	0.65	0.2	8×10^2	1	1	0.001	0.1	20	32
Medium	Walker2d	2×10^{-4}	0.65	0.2	4×10^2	1	1	0.01	0.1	20	32
Med-Replay	HalfCheetah	2×10^{-4}	0.65	0.4	1×10^8	1	1	0.1	0.001	20	4
Med-Replay	Hopper	2×10^{-4}	0.55	0.2	9×10^2	1	1	0.001	0.1	20	32
Med-Replay	Walker2d	2×10^{-4}	0.6	0.05	1×10^8	1	1	0.1	0.1	20	32
U-Maze	Maze2d	2×10^{-4}	5	0.2	1×10^8	1	1	0.1	-	20	128
Medium	Maze2d	2×10^{-4}	0.1	0.02	1×10^8	1	1	0.1	-	20	256
Large	Maze2d	2×10^{-4}	0.6	0.01	1×10^8	1	1	0.1	-	20	384

$$\nabla \theta = \frac{\partial \mathcal{L}}{\partial \theta} \quad (18)$$

$$= \lambda_d \frac{\partial \mathcal{L}_d}{\partial \theta} + \lambda_v \frac{\partial \mathcal{L}_v}{\partial \theta} + \lambda_c \frac{\partial \mathcal{L}_c}{\partial \theta} \quad (19)$$

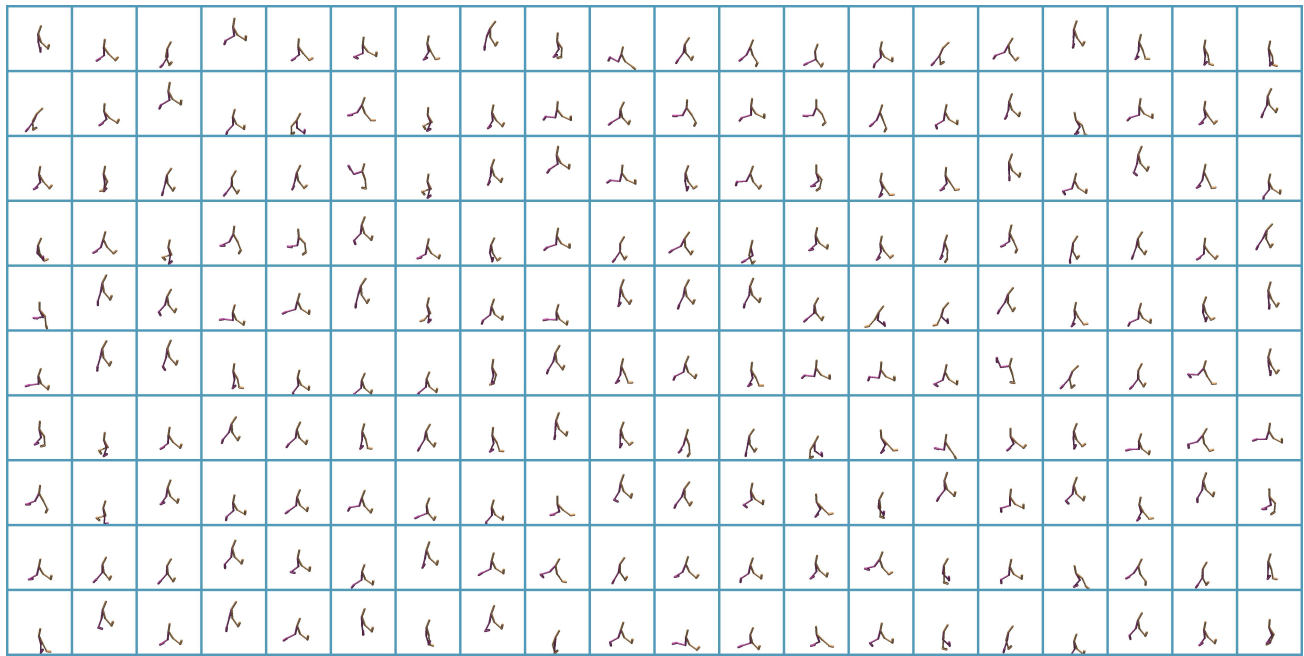
$$= \lambda_v \frac{\partial \mathcal{L}_v}{\partial \theta} + \lambda_c \frac{\partial \mathcal{L}_c}{\partial \theta}, \quad (20)$$

$$\nabla \phi = \frac{\partial \mathcal{L}}{\partial \phi} \quad (21)$$

$$= \lambda_d \frac{\partial \mathcal{L}_d}{\partial \phi} + \lambda_v \frac{\partial \mathcal{L}_v}{\partial \phi} + \lambda_c \frac{\partial \mathcal{L}_c}{\partial \phi} \quad (22)$$

$$= \lambda_d \frac{\partial \mathcal{L}_d}{\partial \phi}. \quad (23)$$

Thus, calculating the gradients of θ with \mathcal{L} is equal to calculate θ with \mathcal{L}_d and \mathcal{L}_c , calculating the gradients of ϕ with \mathcal{L} is equal to calculate ϕ with \mathcal{L}_v , *i.e.*, optimizing the return predictor $\mathcal{J}\phi(\cdot, \cdot)$ with Equation (14) is equal to optimizing it with Equation (12) only.



(a) Agents with high-return states.



(b) Agents with low-return states.

Figure 10. Visualization of positive samples (states with high returns) and negative samples (states with low returns) in Walker2d-Med-Replay.